

Quantitative chemical tagging, stellar ages and the chemo-dynamical evolution of the Galactic disc

A. W. Mutschang^{1,2} \star , G. De Silva³, D. B. Zucker^{1,2,3}, B. Anguiano^{1,2}, T. Bensby⁴, S. Feltzing⁴

¹ Macquarie University Research Centre in Astronomy, Astrophysics & Astrophotonics, NSW 2109, Australia

² Department of Physics & Astronomy, Macquarie University, NSW 2109, Australia

³ Australian Astronomical Observatory, PO Box 296, NSW 1710, Australia

⁴ Lund Observatory, Department of Astronomy and Theoretical Physics, Box 43, SE-221 00 Lund, Sweden

8 October 2018

ABSTRACT

The early science results from the new generation of high-resolution stellar spectroscopic surveys, such as GALAH and the Gaia-ESO survey, will represent major milestones in the quest to chemically tag the Galaxy. Yet this technique to reconstruct dispersed coeval stellar groups has remained largely untested until recently. We build on previous work that developed an empirical chemical tagging probability function, which describes the likelihood that two field stars are conatal, that is, they were formed in the same cluster environment. In this work we perform the first ever blind chemical tagging experiment, i.e., tagging stars with no known or otherwise discernable associations, on a sample of 714 disc field stars with a number of high quality high resolution homogeneous metal abundance measurements. We present evidence that chemical tagging of field stars does identify coeval groups of stars, yet these groups may not represent distinct formation sites, e.g. as in dissolved open clusters, as previously thought. Our results point to several important conclusions, among them that group finding will be limited strictly to chemical abundance space, e.g. stellar ages, kinematics, colors, temperature and surface gravity do not enhance the detectability of groups. We also demonstrate that in addition to its role in probing the chemical enrichment and kinematic history of the Galactic disc, chemical tagging represents a powerful new stellar age determination technique.

Key words: stars: abundances – Galaxy: open clusters and associations: general – techniques: miscellaneous (chemical tagging) – Galaxy: disc – Galaxy: evolution

1 INTRODUCTION

The field of Galactic Archaeology, aimed at uncovering the events that led to the current state of the Milky Way – and more broadly to spiral galaxies in general – harnesses the unique observational property of our own Galaxy: that we can resolve individual stars. Though many large photometric surveys have taken advantage of this, to date there have been few large scale spectroscopic surveys observing Milky Way stars. Notably, the SEGUE (Yanny et al. 2009) and RAVE (Steinmetz et al. 2006) surveys have enabled important advancements in the understanding of the dynamical nature of the Galaxy. Both surveys were done at low resolution; high resolution counterparts at the same scale have yet to come. However, this is set to change in the coming years, as the Gaia-ESO public spectroscopic survey (Gilmore et al. 2012) continues observations of upwards of 100 000 stars, and the unprecedented million star survey, GALAH (Galactic Archaeology with HERMES;

Freeman et al. 2013) begins operations at the Anglo-Australian Astronomical Telescope (AAT) in late 2013. Combined with the precise astrometry of the Gaia space telescope mission¹, we will soon have an extremely detailed and comprehensive picture of millions of Galactic stars.

Of great importance to the study of the evolution of the Galaxy as a whole is the chemical and kinematic evolution of the disc. The disc is where most star formation occurs, it is rich with astrophysical fossils and is relatively easy to observe (compared to the stellar halo or bulge/bar). A common view of the physical structure of the Galaxy is that there are two major components of the disc: a thick, diffuse disc with a scale height of order 1 kiloparsec, and a compact and dense thin component with a scale height of about 300 parsecs (Gilmore & Reid 1983). In this paradigm, the thick disc stars are old, metal poor, and have large dispersions in their vertical space motions. The thin disc, on the other hand, is young, metal rich,

\star E-mail: arik.mutschang@mq.edu.au

¹ <http://sci.esa.int/gaia>

and has a small vertical velocity dispersion (Bensby et al. 2003; Nordström et al. 2004; Bensby et al. 2005; Anguiano et al. 2013). A healthy debate continues as to the origin of the thick disc. Is it a product of a galactic collision or tidal interactions with dwarf galaxies (Quinn et al. 1993; Abadi et al. 2003)? Or does the process of stellar radial migration (Sellwood & Binney 2002; Minchev et al. 2011; Loebman et al. 2011; Roškar et al. 2013) play a dominant role in the kinematic heating? Perhaps none of these explains the existence of the thick disc. Another paradigm for describing the Galactic disc as a whole is that, instead of two monolithic components with distinct evolutionary paths, there is a smooth distribution of “mono-abundance populations” (MAPs) which rise out of constant heating and star formation cycles (Bovy et al. 2012; Rix & Bovy 2013). To address such questions requires detailed chemical and kinematic analyses of large numbers of stars. Without a doubt, Gaia will accomplish the latter. The former is where GALAH will make great strides.

GALAH is not just a high-resolution spectroscopic survey of a million stars. A primary mission of the survey is to “chemically tag” the entire sample in order to search for long-since-dispersed star clusters. Freeman & Bland-Hawthorn (2002) introduced the concept of chemical tagging, in which stars are linked to individual star formation events when their abundance patterns in a range of elements, from α to Fe-peak, light to heavy s and r-process, are the same. This is possible, in theory, because star formation within clusters occurs in rapid bursts within a giant molecular cloud which is well mixed with enriched material from a previous generation of stars. It is thought that all stars in the Galaxy are formed within such clusters and disperse on time-scales of typically tens to several hundred Myr in the Solar neighborhood (Janes et al. 1988; Lada & Lada 2003). The chemically tagged stars then would be considered *conatal*, or having formed in the same molecular cloud, localised within the Galactic disc, implying also that they are *coeval*, having formed at the same epoch.

For chemical tagging to work in practice, it is important that star clusters that represent typical star formation (insofar as possible) be homogeneous in their abundance patterns. Open clusters and moving groups have been shown to exhibit uniform abundance patterns based on high resolution, high signal-to-noise abundance analyses (De Silva et al. 2006, 2007a,b; Bubar & King 2010; Pancino et al. 2010). In addition to the requirement of homogeneity within open clusters, chemical tagging relies on the adequate differentiation of distinct clusters in abundance space. Recently, Mitschang et al. (2013) used a high resolution spectroscopic sample of Galactic open cluster stars from the literature to quantify the level to which chemical tagging can distinguish between conatal and disparate stars. They developed a chemical difference metric, δ_C , which decomposes the N-dimensional chemical abundance space. An empirical probability function was derived, which allows confident tagging of pairs of stars using the δ_C metric. The dimensionality of chemical tagging abundance space has also been probed. Ting et al. (2012) used a principal component abundance analysis (PCAA) to discover the elements with the largest global variance, finding 8-9 elements form a truly independent set. These will be the most powerful chemical tags and will be the target of chemical tagging surveys.

There have been several studies applying the concepts of chemical tagging on small scales. De Silva et al. (2011) and Tabernero et al. (2012) used chemical information to make membership decisions on stars compatible with the Hyades supercluster association, as did Pompéia et al. (2011) with the Hyades stream to test its origin. De Silva et al. (2013) found that the Argus asso-

ciation stars probably originated from the open cluster IC 2391, using chemical tagging supported by kinematic and chronological information. Conversely, Carretta et al. (2012) found chemical information from a handful of elements indicated several distinct populations in the open cluster NGC 6752. Beyond the Galaxy, but still within reach of current instrumental capabilities, even coeval groups in a dwarf galaxy have been tagged using chemical information (Karlsson et al. 2012). It is important to note that these studies were able to make qualitative decisions based on chemical signatures due to *a priori* information on their likelihood of membership in an association. There will be no such advantage for a large scale chemical tagging experiment looking for dispersed coeval structures. To date, no *blind* chemical tagging experiment, one where the sample stars have no known associations, has been carried out; this is the goal of the current work.

In the context of Galactic evolution, accurate ages must play an integral role. Stellar ages, however, are notoriously difficult to infer for single stars (see Soderblom 2010 for a comprehensive review). The most common method, isochrone fitting, has significant limitations, and although astroseismology can produce very accurate ages, it takes significant observational investment and may not yet be appropriate for all stars (Soderblom 2010). An important point is that, aside from the Sun, the most accurate ages, and those which set the basis for statistical age relations and stellar model calibrations, are those from open clusters (conatal and coeval stellar groups).

In this paper we aim to characterise chemical tagging via the group finding technique from Mitschang et al. (2013), conducting the first blind chemical tagging experiment at any scale. We show that results from the chemical tagging are consistent with appropriate coeval linking based on several indicators, but that information classically used as membership indicators in conatal groups (open clusters), e.g. velocity dispersions, photometric colors and magnitudes, surface gravity and effective temperatures, etc., will not typically aid in identifying contaminated groupings. The *predictions* section in Soderblom (2010) does not mention chemical tagging as a future source of stellar age determination, yet we argue here that this is amongst the most important outcomes these experiments will yield. That is, instead of independently measured stellar ages being used to scrutinize the tagging of coeval groups, rather chemical tagging will produce more accurate and precise ages for a larger number of stars than otherwise would be possible.

2 DISC FIELD CHEMICAL ABUNDANCE DATA

We perform our chemical tagging experiment on a large sample of 714 disc field dwarfs and subgiants, observed using the high-resolution spectrographs FEROS at the ESO 1.5m and ESO 2.2m telescopes, SOFIN at the NOT, MIKE at the Magellan Clay telescope, and UVES at the ESO VLT telescope. Typical resolutions of these observations range between $R=42,000$ to $110,000$, and signal-to-noise ratios are typically above 250. The analysis of the spectra, including computing stellar parameters and element abundances is described in Bensby et al. (2013).

This homogeneous abundance sample of mostly dwarf and turn-off stars inhabits a volume with an approximately 150 parsec radius centred on the Sun. All 714 stars have trigonometric parallaxes and proper motions taken from the TYCHO-2 catalogue (Høg et al. 2000), so in addition to the 12 dimensional chemical abundance space comprised of Fe, Na, Mg, Al, Si, Ca, Ti, Cr, Ni, Zn, Y, Ba, we also have 6 dimensions of position and kinematic

space. Ages for individual stars in this sample have been derived using an isochrone fitting method described in [Bensby et al. \(2011\)](#). The high precision in the analysis and chemical dimensionality (see, e.g., [Ting et al. 2012](#); [Mitschang et al. 2013](#)) along with the size of this sample make it an ideal data-set for the first truly blind chemical tagging experiment.

3 CHEMICAL TAGGING

3.1 Group finding procedure

We performed group finding using the algorithm described in [Mitschang et al. \(2013\)](#). The procedure works by computing the pairwise metric δ_C defined as

$$\delta_C = \sum_C \omega_C \frac{|A_C^i - A_C^j|}{N_C}$$

where N_C is the number of measured abundances and A_C^i and A_C^j are individual abundances of element C for stars i and j, respectively. The ω_C factor may be used to give more or less weight to a particular element, with respect to the overall chemical difference, given some external knowledge about that element. In this case, given the lack of detailed study into this factor, we fix it at unity for all elements involved in the δ_C computation. This metric is then computed over all pairs of stars, describing the difference in abundance patterns of those particular stars.

Then, utilizing the empirical probability function based on open clusters derived in [Mitschang et al. \(2013\)](#), the δ_C values are translated to a probability, P_{lim} that a given pair i and j are conatal (i.e. formed in open cluster-like star formation events). Simply understanding if two stars have a reasonable chance of being conatal is interesting, but we seek to find groups that have a high *combined* probability, essentially reassembling a long-since dispersed cluster of stars.

Our algorithm for linking groups begins with the highest density clustering in δ_C space and assembles groups such that all star pairs meet the required probability threshold. Briefly, the algorithm proceeds as follows: all pairs for which the probability is less than our threshold are first removed, and the remainder sorted by highest probability first. Chemically tagged groups of stars are formed by linking pairs that share common stars such that an individual star only inhabits one cluster. The sorting ensures only the best match for pairs that may adequately match more than a single group. Linking then proceeds down the chain of pairs, removing those pairs where one of the stars has been assigned to a group. We did this for two values of limiting probability, P_{lim} , of 90 and 68%. The 68% threshold, corresponding to approximately a 1- σ detection of the coeval signature between two stars, is the lowest meaningful probability we can tag with, yet at a δ_C of 0.057 dex we are pushing the limits in terms of abundance measurement uncertainties.

The sample used for calibration of the chemical tagging probability function was selected from high-resolution studies with uncertainties on the order of the current sample. Therefore, with respect to internal errors, the function is appropriately applied to this study at the 68% level. The effects of systematic uncertainties due to the heterogeneous calibration sample are discussed in detail in [Mitschang et al. \(2013\)](#); here we note that the 90% threshold also explored in the current work corresponds well to the 68% threshold in the simulated ‘‘intrinsic’’ probability function, which attempts to weigh the contribution of external uncertainties. This can be under-

Table 1. The properties of groups recovered for various probability levels.

P_{lim}	68%	68% $N_{*}>2$	90%	90% $N_{*}>2$
δ_C lim (dex)	0.057		0.033	
Num clusters	102	67	171	80
Mean δ_C^{avg} (dex)	0.039	0.037	0.025	0.024
Min δ_C^{avg} (dex)	0.026	0.026	0.011	0.015
Mean N_*	6.6	8.9	3.0	4.2
Max N_*	42		12	
% tagged	94	84	73	47

Table 2. Group linking between stars at 68% probability detection threshold. The full version of this table is available with the arXiv source files (table_2.dat).

HIP	GID
80	6
305	13
407	1
699	18
768	19
:	:
:	:

stood, loosely and in a global sense, as indicative of the errors on group determination.

The results of group linking are summarised in [Table 1](#). For each threshold we list the corresponding limit in δ_C taken from the probability function (δ_C lim), the number of groups recovered for which there were at least three members (Num), the mean δ_C^{avg} (δ_C^{avg} is the average of pair probabilities over the recovered group), the mean and maximum number of stars in the detections and the percentage of all stars in our sample that were tagged to groups.

The link between stars and groups identified at the 68% probability level is given in [Table 2](#), where each star identified as part of a group with 3 or more members has its Hipparcos number (HIP) listed along with a group identification number (GID).

3.2 Results of group finding

The distribution of member counts per group and their respective average δ_C values are shown in [Figure 1](#). Note the exponential drop off in the number of recovered members; a majority of the groups have no more than 4 members. At $P_{lim} = 68\%$, the largest group has 38 members, and also exhibits one of the smallest mean δ_C values (or high mean pair probabilities). Indeed, we see a slight rising trend in mean δ_C with increasing member counts for both probability thresholds in the lower panel of [Figure 1](#). To some degree, this is explained by our algorithm’s preference for the highest density groups (those having smallest δ_C), which are linked first.

Amongst the recovered coeval groups there is a wide variety of properties of the members in terms of stellar parameters, e.g. surface gravity, effective temperature, space velocities, abundance patterns and ages. There is over one dex of variation in the metallicities between groups, yet all of them, by definition, have homogeneous abundance patterns. Such diversity in a modest sample of stars as in this study affords an excellent opportunity to not only study chemical tagging, but also the science it will enable. [Figure 2](#) shows four examples from the $P_{lim} = 68\%$ set showing orientations in three kinematic planes (U, V, and W) and $\log g$ vs. T_{eff}

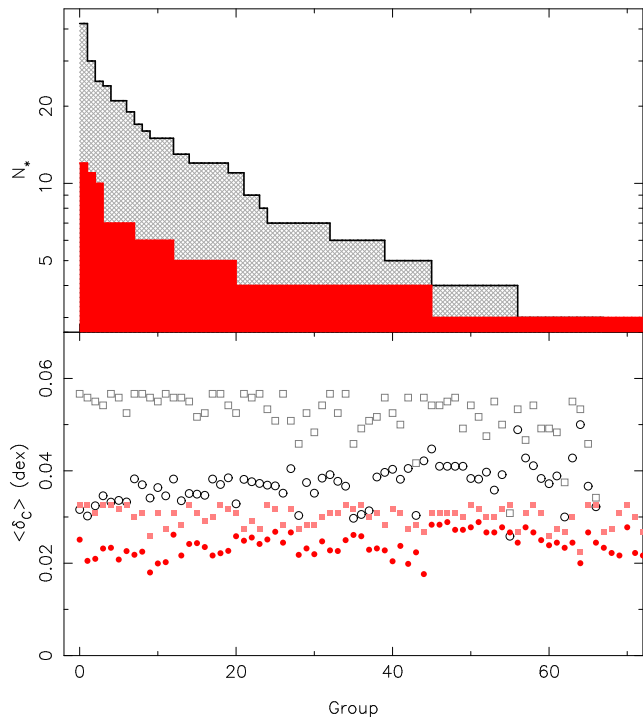


Figure 1. The top panel shows the distribution of numbers of members for groups with 3 or more members, while the bottom panel shows the δ_C values corresponding to the bins; squares are the max δ_C and circles are the mean, in each group. Both panels are sorted by number of stars in the recovered group. In each panel $P_{lim} = 90\%$ is represented by red, while $P_{lim} = 68\%$ is black.

planes, with comparison to the entire sample, selected to illustrate some of the range, and extremes, of recovered groups. Panel (a) shows one of the largest tagged groups, which, though it exhibits large scatter in kinematics, has a tight orientation in the CMD plane about its best-fitting isochrone (see Section 4). In panel (c), the main sequence of the group appears atypical by eye, given the a seeming reverse slope, and is difficult to fit due to this and the predominance of lower main-sequence dwarf stars, an issue which affects many groups in the analysis (seen in panel d as well); stars on the lower main-sequence provide only weak discriminatory power between isochrones of different ages, due to the convergence of evolutionary tracks at low surface gravities. However, it is important to note that the atypical form may be an illusion; if the full population of that group were available, it is possible the same interpretation would not be made, perhaps save a single star. Panel (d) shows a low membership group where mostly lower main-sequence stars are identified, consequently making an age determined from it less meaningful. Figure 2 also highlights the range of ages that the groups have from under one to 14 Gyrs.

Performing the calculation for total chemical tagging efficiency given in Mitschang et al. (2013), based on their literature abundance sample, the expected efficiency of chemical tagging at 68% limiting probability would be roughly 9%, meaning that 9% of the total sample of stars could be reliably tagged. Combining the contamination rate of 50% in that study with the $\sim 80\%$ tagged in our experiment, we may have cleanly tagged 40% of the stars in our sample, which is significantly larger than expectations. Moreover, the 9% efficiency estimate was based purely on the confluence of two separate star formation signatures in chemical space, due to the fact that the abundance sample used contained only stars from

known open clusters. A field star sample would be further complicated by dynamical mixing processes, which means that the chemical tagging efficiency would have to be folded in with the prior probability that any two random stars in a local sample, regardless of their observed properties, are conatal. In this context, the number of stars tagged seems at odds with the number of conatal signatures we might expect. How likely is it that we would find multiple (or any) such conatal associations in the Hipparcos volume?

A comprehensive approach to answering that question would require detailed modeling of Galactic evolution at the scale of individual stars, tracking disrupting clusters over a large range of cosmic time, possibly in the form of an N-body simulation. To our knowledge, simulations of this nature have not been fully rendered yet.

In Freeman & Bland-Hawthorn (2002) it is suggested that chemical tagging will probe particular enrichment events, i.e., those which polluted a molecular cloud resulting in a star formation episode discrete in space and time. Those stars would then disperse around the Galaxy, retaining their initial chemical patterns. Given the seeming implausibility of detecting as many apparent coeval groups as we have, even for very tight chemical differences, we offer several interpretations that may explain our results:

- 1.) The chemical overlap between conatal groups is far greater than observed in Mitschang et al. (2013), resulting in high contamination, and tagged groups represent nothing more than stars with similar chemistry.
- 2.) Open clusters, or the current literature sample, do not adequately represent typical star formation in the disc, resulting in the contamination estimate being either too high or too low.
- 3.) Stellar dynamical mixing processes (e.g. radial migration, churning) are not efficient, keeping members of unbound associations in relative proximity.
- 4.) The star-formation and enrichment cycle, per epoch, is not stochastic, yielding similar abundance patterns as a function of age to within current measurement abilities. In other words, chemically tagged groups represent coeval, but *not* conatal, stars.

We will continue to discuss these interpretations of chemically tagging groups for the remainder of this work. Initially, and for the next section, involving stellar age determinations, we operate on the traditional assumption of Freeman & Bland-Hawthorn (2002), that these groups represent star formation sites similar to open clusters but which have dispersed, i.e., they are considered conatal.

4 STELLAR AGE DETERMINATIONS

Perhaps one of the most powerful incentives to tag coeval groups of stars is to enhance the reliability of determining ages for the stars that make them up. There are many methods for determining ages for single stars (Soderblom 2010), but by far the most common method is by fitting isochrones to their positions on a CMD plane. The most obvious difficulty here is that fitting any model curve to a single point is a highly degenerate problem. With isochrones, this is especially difficult in the lower main-sequence region, as tracks of different ages converge with decreasing temperature on the main sequence. Even in the turn-off region, where the track separation is higher for any given difference in age, overlaps can resurface at very large age separations.

More subtly, these fitting procedures aim to land the star exactly on the isochrone. It is possible that scatter about model

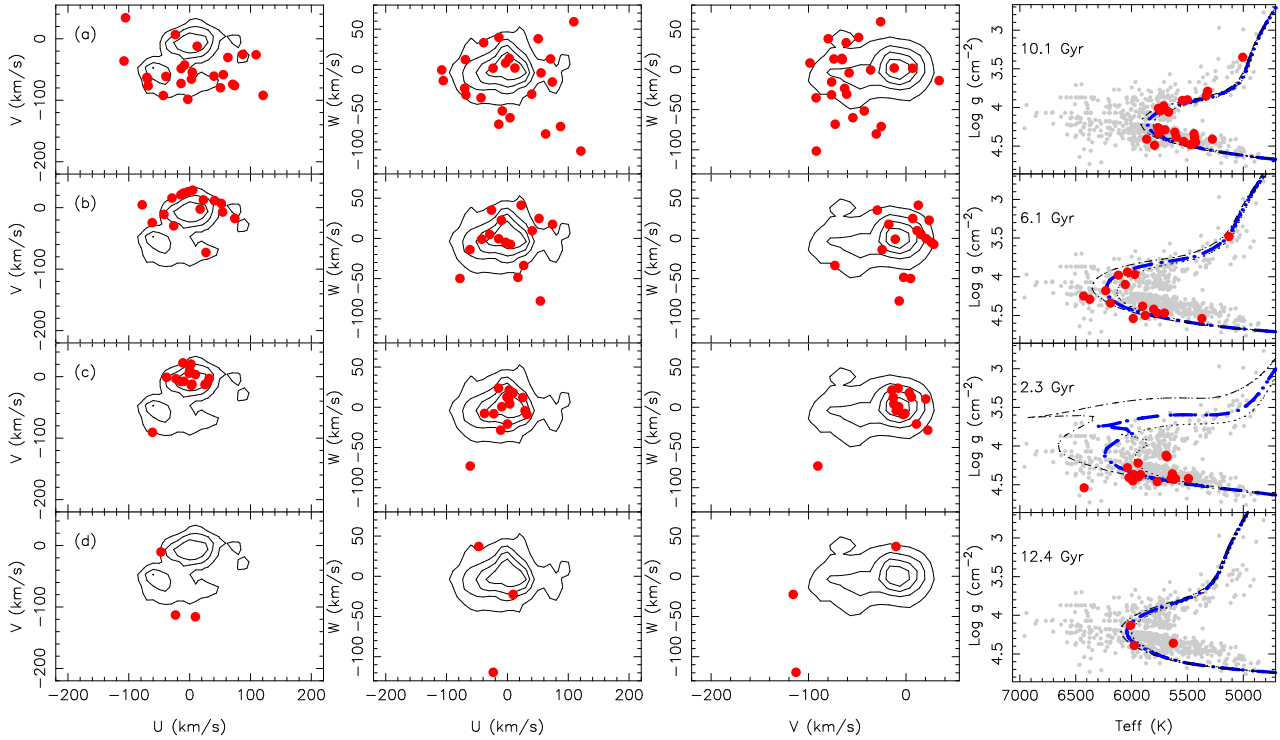


Figure 2. UV, UW and VW kinematic plots for a sample of recovered groups along with T_{eff} and $\text{Log } g$ CMD plots. The kinematic plots show the entire sample in black contours and members with red circles. The CMD plots show the entire sample in grey points, the member stars in red circles and the best-fitting isochrone to the group as a dashed blue line. The dot-dashed and dotted black lines are isochrones one Gyr younger and one Gyr older, respectively, for comparison. These groups were selected to illustrate the wide variety, and extremes, of kinematic and CMD orientations that are present in our recovered groups.

isochrones exists beyond the measurement errors for open cluster stars. If it is true that open clusters form quite rapidly (e.g., see Lada & Lada 2003), and that a single isochrone describes the population well, then that scatter must be due to parameters other than age, e.g. metallicity inhomogeneity, intrinsic variations in stellar atmospheres, or some other not well understood or accounted for physics of stellar evolution. This implies, of course, that a single star age, even on the main sequence turn-off, can differ significantly to that more appropriately determined via fitting of its coeval siblings. In this section, we describe our procedure for fitting isochrones to determine ages for chemically tagged groups.

4.1 Isochrone fits

We used the Yale-Yonsei version 2 (Y^2 ; Demarque et al. 2004) isochrone sets in fitting all chemically tagged groups. In order to best tune our determinations, we generated an interpolated grid of isochrones, using the supplied YYMIX2 Fortran code, with a resolution of 100 Myr in age from 0 to 14 Gyr, and 0.01 dex in both $[\text{Fe}/\text{H}]$ and $[\alpha/\text{Fe}]$, each covering the entire range of abundances in our data.

Best-fitting isochrones for each group were computed from the resultant three dimensional grid automatically using a least squares method. Figure 3 shows the results of isochrone fitting for a typical chemically tagged group. It is evident from the scatter in the members that isochrone fits to individuals would result in incompatible ages. However, the magnitude of scatter is actually typical of conatal groups. The shaded square symbols show stars of HR1614 from De Silva et al. (2007b), a well studied moving group

that is thought to be a dissolving conatal group of stars (see also Feltzing & Holmberg 2000). Note the scatter of HR1614 members about its best-fitting isochrone. Comparing that to the overall scatter of the entire stellar sample (shown in light gray triangles) implies that, in many cases, stellar parameters (e.g. color, magnitude, temperature, surface gravity) do not add dimensionality to group finding using chemical tagging. In other words, chemically tagged groups in general will not be further refined via the position of their members in the CMD. Inspection of CMDs in our sample confirmed this; only in a few cases (<10%) did we find obvious incompatible arrangements (i.e., stars that appear well away from the bulk of the group, in a way that would not satisfy stellar evolution tracks, taking into account acceptable scatter in this plane; see e.g. (b) of Figure 2).

4.2 Age uncertainties

Uncertainties in our age determinations are related to uncertainties in effective temperature and surface gravity measurements for individual stars, and for group mean uncertainties on the interpolation parameters $[\text{Fe}/\text{H}]$ and $[\alpha/\text{Fe}]$. Because $[\alpha/\text{Fe}]$ was calculated by proxy, by the averaging of abundances for Ti, Mg, Si, and Ca resulting in relatively small errors, and the effect of modulation of this parameter on the isochrone is minimal compared to that of $[\text{Fe}/\text{H}]$, we ignored it in our error calculations.

In estimating uncertainties, we employed a Monte-Carlo approach where each simulation iteration consisted of randomly redistributing the stars in T_{eff} and $\text{Log } g$ by a factor between zero and unity times their individual uncertainties on those parameters,

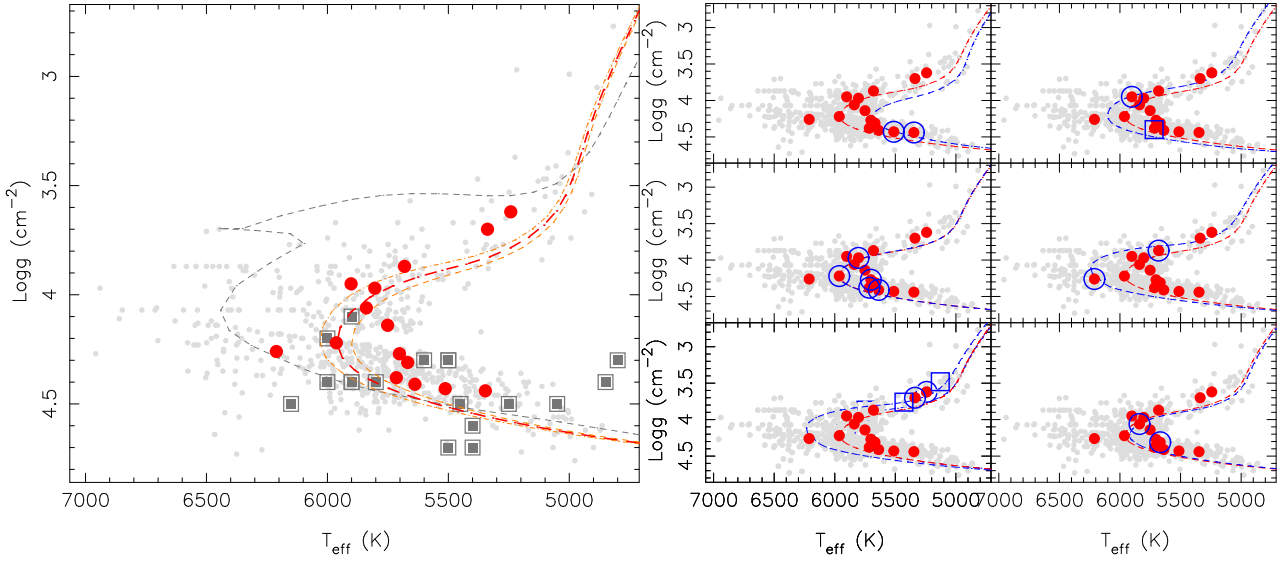


Figure 3. Detailed view of CMD for a single group. The left hand panel shows the CMD for a group consisting of 15 members tagged to the 68% probability threshold (red filled circles). The red dashed line shows its best-fitting isochrone, while dash-dot and dashed orange lines are best-fitting minus and plus one Gyr, respectively. Also shown are all stars in the sample for reference (light gray points), and HR1614 member stars from [De Silva et al. \(2007b\)](#) (grey squares), along with its best-fitting 2 Gyr isochrone (grey dashed line). The HR1614 stars and isochrone serve to illustrate typical levels of scatter observed in conatal groups. The right hand panel shows 6 sub-groups, tagged at the 90% probability threshold, that comprise the same group at the 68% level. Symbols are as in the left panel, blue open symbols represent each sub-group, and the blue dashed line is the best-fit isochrone of that sub-group. Note that some subgroups have additional stars not tagged at the lower probability level (blue squares).

and re-evaluating the best-fitting. The size of each simulation set was chosen to be 1000 and each set was repeated three times for the cluster mean $[\text{Fe}/\text{H}]$, $[\text{Fe}/\text{H}] - \sigma[\text{Fe}/\text{H}]$ and $[\text{Fe}/\text{H}] + \sigma[\text{Fe}/\text{H}]$, resulting in a distribution of 3000 ages for each recovered group. The 1σ uncertainty limits on the distribution for each group were taken as its age errors, which are shown in the right panel of Figure 4 in comparison to those from single star ages.

Of course, there must be uncertainties related to our membership determinations. The effects of sub-sampling a coeval group of stars and fragmentation from group finding (e.g. due to higher P_{lim}) are discussed in more detail in Section 4.3; however, for the following reasons we ignore these complicated sources of error in this discussion. Because the sub-sampling effect has a greater impact at the measurement of a single star, our calculated uncertainties actually represent *upper limits* when making comparisons to those from single stars. Similarly, because uncertainties on single stars ignore intrinsic scatter in their calculations, i.e. they only take into account uncertainties on measured parameters, they can be thought of as representing *lower limits* of the true uncertainty. Finally, as we aim to characterize chemical tagging and study the validity of groups derived therefrom, we must rely the assumption that our group determinations are correct, and contamination is represented by statistical deviations in the relations and quantities we derive.

4.3 Fragmentation

We now explore the issue of fragmentation in coeval groups linked via chemical tagging. Fragmentation, as discussed here, is the sub-sampling of a single chemically tagged group that is caused by tagging at higher probabilities. In observational studies of stellar populations we are almost always sub-sampling, or observing only a fraction of, the whole underlying population. In chemical tagging, effects related to this are especially important both due to the small numbers in tagged groups, and the trade-off between high

pair probabilities within groups and the accuracy of ages determined from them.

The right hand panel of Figure 3 shows the fragmentation of a single 18 member group, as tagged to the 68% probability, when tagged at the higher probability of 90%. The fragmented groups in the middle left and upper right plots exhibit noticeable discrepancies between their best-fitting isochrones (shown in blue dashed line) and that of the larger group, while the others are more generally consistent. The mean and maximum absolute age differences between the fragments and the “parent” group, at 1.6 Gyr and 4.7 Gyr, respectively, are less than the same quantities compared to the ages derived for single stars, at 2.9 Gyr and 6.4 Gyr. It is impossible in a blind chemical tagging experiment to determine which of these fragments are truly parts of the same population, and to what extent contamination is affecting the particular group at lower probabilities. It is somewhat reassuring, however, that the mean differences in age between stars calculated from groups at the 68% and 90% levels, for the entire sample, of 1.2 Gyr is close to the typical uncertainties computed as above, and lower than the mean difference between single star ages and those calculated for stars tagged to 68% probability of 1.7 Gyr.

As seen in Figure 1, a large fraction of groups have few members. Even in the (presumably rare) case that one of these groups has absolutely no contamination, the age we calculate for it will be affected by the inherent sub-sampling of observational studies. The severity of this effect is proportional to the sub-sample size, thus these small groups present additional challenges, on top of the uncertainties associated with chemical tagging. In an attempt to quantify the magnitude of this effect on a chemical tagging experiment such as this, we simulated sub-sampling of the Hyades cluster (from [Tabernero et al. 2012](#)) for sub-samples sized from 3 to 27 members (the full sample having 28 stars), representing the range of coeval group populations found in this study. Each simulation iteration selects a random sub-set of N stars from the Hyades mem-

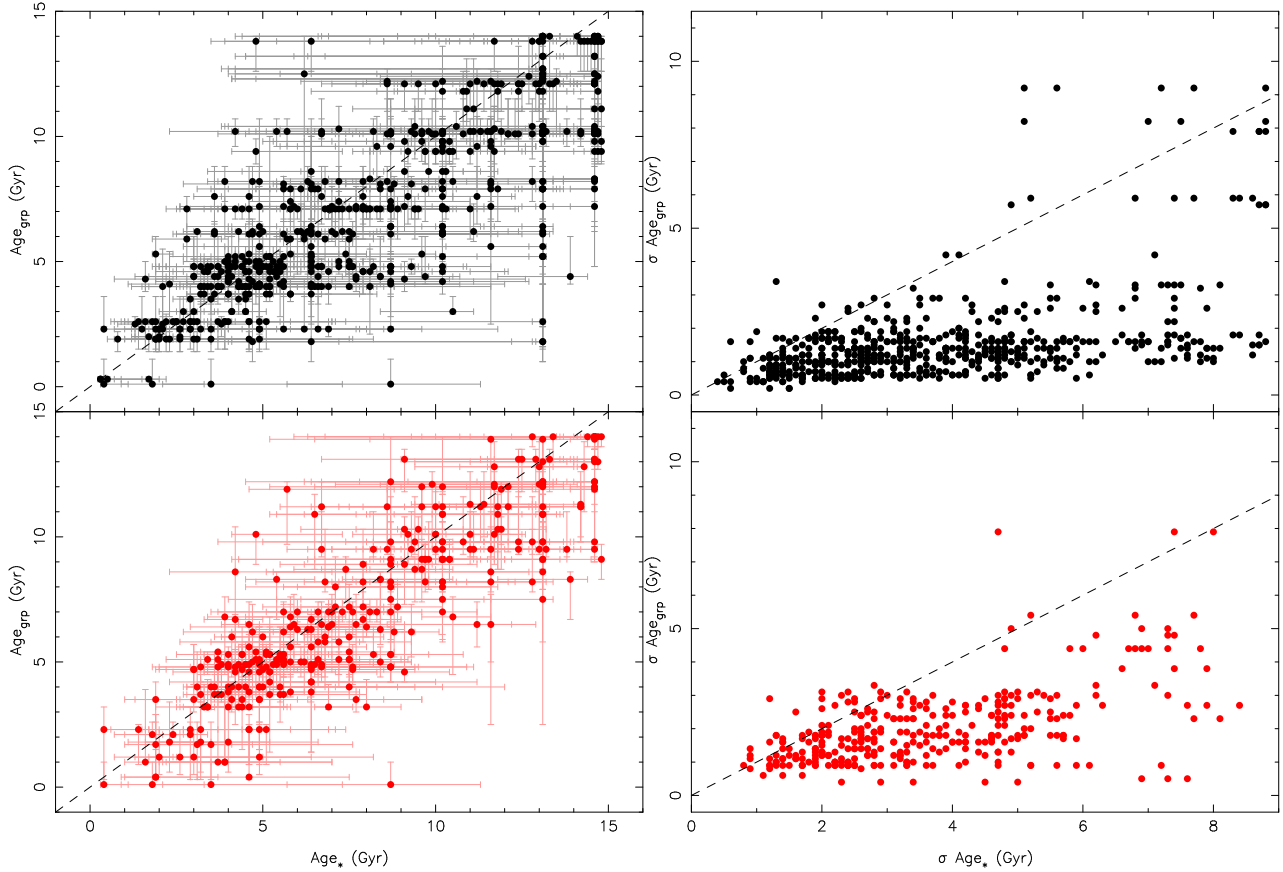


Figure 4. Ages fit for individual stars vs those fit for clusters identified by chemical tagging. Equality is indicated by the dashed line in each panel. The top panels show members of groups at a limiting probability of 68%, while the bottom panel shows a limiting probability of 90%. The left hand panels show comparison of ages while the right hand panels show comparison of the uncertainties on age. Note the difference in proportion of small groups between the two tagging thresholds, and the increase in scatter of the errors. In general, however, the group determined age errors are lower.

bers, and computes the age by best-fitting isochrone. We performed 1000 realizations of this simulation for each size, and computed the difference of the mean age to that of the Hyades, and the dispersion of ages in the simulated sets, as shown in Figure 5. This simulation was repeated with the condition that one of the sub-sample members is more evolved than a dwarf star (dashed lines in Figure 5), which results in improved age constraints.

The results are much as expected, with a clear trend for more accurate ages as sub-sampling size increases. The dispersion within simulation iterations can be thought of as a fundamental uncertainty, not related to the accuracy of measured quantities, but rather to how well the observed sample represents the population as a whole. With sub-giants required as members, the accuracy (mean) substantially improves, while the precision (dispersion) improves to a lesser degree. In addition to providing context to the meaning of age determinations, these results indicate the importance of large sample sizes for chemical tagging.

4.4 Comparison to single star ages

The isochrone fitting procedure described above was completed for all chemically tagged groups. The results are shown in Figures 4, and 6. The former shows a direct comparison between single star ages and chemically tagged ages in the left hand plot. A general agreement exists, yet there is significant scatter and a tendency for single star ages to be larger than the respective group ages. Depart-

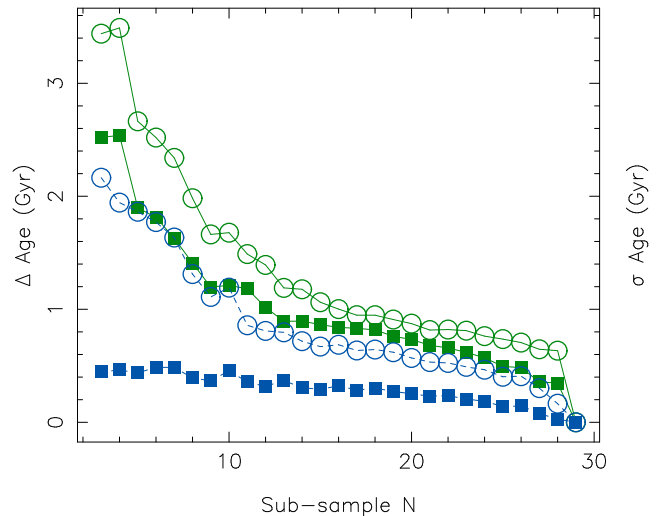


Figure 5. Sub-sampling simulations of the Hyades. The green squares-line is the difference of the simulation mean age to the age of the Hyades, the green circles-line is the dispersion of ages in the simulated sets, as a function of sub-sample group size. The corresponding dashed blue lines are for simulations where we guaranteed at least a single sub-giant star. The results are much as expected, with the accuracy of measurement increasing with increasing sample size.

tures from a one to one relationship between age determinations are also common in our results, with a slight tendency for turn-off and sub-giant branch stars to have greater agreement between methods.

Figure 6 shows the scatter of single star ages within coeval groups. Each bin in the filled histograms represents the number of groups where the single star ages exhibit the dispersion indicated. The line plots show the breadth of age differences in the groups. This is defined as the difference between the largest and smallest single star age within a group. The mean dispersion of over ~ 2 Gyr (in the $P_{lim} = 68\%$ case) suggests the prospects of using ages determined through isochrone fitting of individual stars as an added group finding dimension are fairly poor. Dispersions over 6 Gyr are seen, and the breadth of disagreement extends well past 10 Gyr. If we extend the distribution of groups found herein to a much larger sample (e.g. a million stars) this will amount to a significant number of coeval groups with very large dispersions in single star ages.

Though the accuracy of age determinations via chemical tagging is difficult to quantify, being dependent on the accuracy of the group finding, the precision can easily be compared to that of single stars. The improvement in precision of chemically tagged ages over single star ages is illustrated in the right panel of Figure 4, which shows the uncertainties on age derived from the single star method compared with those from the chemically tagged groups. The improvement can be quite substantial – even order of magnitude differences are seen – and is evidently non-linear, due to the variety of arrangements on the CMD plane afforded by multiple stars.

5 AGE TRENDS IN CHEMICALLY TAGGED GROUPS

5.1 Age velocity relations

The groups we have identified via chemical tagging do not unambiguously exhibit clustering in Galactic kinematic (UVW) space (as shown in Figure 2). Given a typical cluster lifetime (i.e. before total dissolution) of on order 10-100 Myr (Janes et al. 1988; Lada & Lada 2003), and an age range on our cluster population from less than 1 to 14 Gyr, there is a proportionally very large span of time for respective members to evolve dynamically within the Galactic environment. The churning and radial migration processes described in Sellwood & Binney (2002) imply that older populations would exhibit greater velocity dispersions. The stochastic nature of the churning process, however, would cause the relationship between velocity and age to loosen for older epochs, unfortunately making kinematics a poorly constrained dimension in chemical tagging group detection.

The overall age-velocity trends we observe using chemically tagged ages suggest the validity of this picture. Figure 7 shows age-velocity relations (AVRs) for all three Galactic velocity components, and the total (quadratic mean of the three components). The vertical axis is the velocity dispersion of the component indicated in the plot, and each point is the dispersion between all members of a single group. There is clearly a relation observed in both the total and W components. The V and U components may similarly exhibit relations, but the scatter is significant, particularly in the U component. Notice also the difference in scale of the top two panels to the bottom two, which is highlighted by the dashed horizontal lines at 50 km s^{-1} .

The existence of a relation in total internal dispersion follows intuitively from star formation scenarios in which clusters

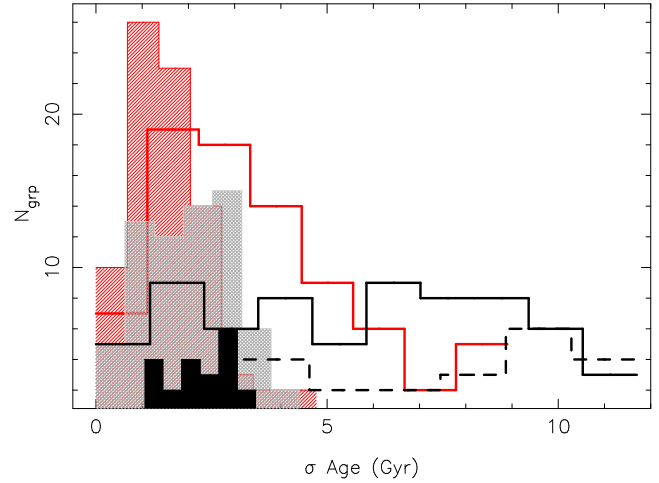


Figure 6. The distribution of scatter of single star age determinations within chemically tagged groups. The grey and red hatched histograms are the dispersions of single star ages within groups from the 68 and 90% pair probability thresholds with 3 or more members, respectively. The filled black histogram shows the 68% case for groups with 10 or more members. The black and red lines show the breadth of age differences within groups for the same thresholds, while the dashed black line shows the same for 68% groups with 10 or more members. The breadth is defined as the difference between maximum and minimum single star age within a chemically tagged group.

disperse on short time-scales. When cluster disruption time-scales are shorter than the dynamical time-scales, older groups would have more time subject to Galactic churning processes than their younger counterparts, and thus exhibit a larger velocity dispersion amongst their constituents. One might expect the terminus of this relation at 0 Gyr to be very close to 0 km s^{-1} , representing the velocity dispersion of the parent molecular cloud at the time of star formation (typically less than $\sim 1 \text{ km s}^{-1}$), however, upon examination of Figure 7 this does not appear to be the case (assuming a linear relation), being somewhere upwards of $\sim 30 \text{ km s}^{-1}$. Assuming the groups are coeval, this result may lend further to option 4 discussed in Section 3.2, because the stars included in the chemically tagged group from distinct *sites* would tend to increase the total dispersion, even at very young ages. In other words, perhaps the AVR indicates that the groups are coeval, but not conatal.

The age-W velocity relation, or disc heating signature, is the most widely studied of these relations. In a dual disc (thick and thin) scenario (e.g. see Gilmore & Reid 1983), the nominal thick disc W dispersion at roughly $\sim 40 \text{ km s}^{-1}$ is higher than the thin by about 20 km s^{-1} . The trends amongst our groups are largely consistent with this picture, showing a smooth heating signature between extremes.

A powerful distinguishing element between the two discs has been shown to be position in the $[\text{Fe}/\text{H}]$ and $[\alpha/\text{Fe}]$ abundance plane, which can either be represented by proxy (in the case of this study, the average of Si, Ti, Ca and Mg), or through individual α elements (Fuhrmann 1998; Feltzing et al. 2003; Bensby et al. 2003, 2005; Reddy et al. 2003, 2006; Navarro et al. 2011). Thick disc stars are typically metal poor and α -enhanced while thin disc stars are metal rich and α -normal. When stars in the group sample are assigned to thin or thick disc based on the following criteria (similar to the Navarro et al. 2011 criteria, but selected on visual inspection of the $[\text{Fe}/\text{H}]$ vs. $[\alpha/\text{Fe}]$ diagram of the present sample):

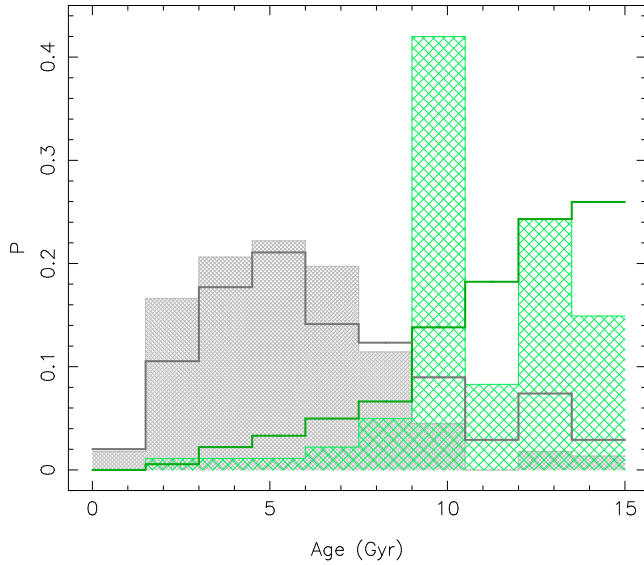


Figure 8. Age distribution functions for the abundance selected thin (grey) and thick (green) discs. The shaded histograms are chemical tagging ages while the solid lines are single star ages – including only stars that are also included in the filled histograms – for reference.

$$\text{Thin disk if } \begin{cases} [\text{Fe}/\text{H}] > -0.6, \\ [\alpha/\text{Fe}] < -0.1 \times [\text{Fe}/\text{H}] + 0.1 \end{cases}$$

$$\text{Thick disk if } \begin{cases} -1 < [\text{Fe}/\text{H}] < -0.1, \\ [\alpha/\text{Fe}] > -0.1 \times [\text{Fe}/\text{H}] + 0.1 \end{cases}$$

we get the age distribution functions for each disc shown in Figure 8. Each component follows a reasonably expected profile, with the thick disc peaking at ~ 10 Gyr while the thin is dominated by stars ~ 5 Gyr old. The tails on chemically tagged age distributions are less prominent than the same distributions using ages derived for single stars, and the thick disc distributions clearly exhibit differing shapes in their profiles towards older epochs. Nevertheless, an important implication here, in agreement with, and perhaps strengthening, conclusions of [Bensby et al. \(2013\)](#), is that stellar age can act as a disc membership discriminant; few thick disc stars should be younger than 9 Gyr, while few thin disc stars should be older.

5.2 Age Metallicity Relation of coeval groups

Stellar elemental abundances as a function of age, the so-called age-metallicity relation (AMR), is the fossil record of the chemical enrichment history of the Galactic disc. This relation is fundamental to a broader understanding of the Galaxy, however, there is not yet agreement on its observational properties (e.g. [Rocha-Pinto et al. 2000](#); [Feltzing et al. 2001](#); [Haywood 2006](#); [Soubiran et al. 2008](#); [Casagrande et al. 2011](#); [Anguiano et al. 2013](#)). The natures of these relations, if indeed they exist, remain uncertain due to the difficulty in obtaining accurate ages for field stars, and the difficulties in defining and observing complete samples.

In Figure 9, we have plotted $[\text{Fe}/\text{H}]$ as a function of chemically tagged ages for coeval groups. The relationship appears roughly linear, while the scatter in metallicity with age, calculated by aver-

aging the dispersion of $[\text{Fe}/\text{H}]$ in 2 Gyr bins, is 0.26 dex, approximately 0.06 dex less than the scatter from single star ages (plotted as light grey dots). The relationship trends from slightly super-solar metallicity for the youngest group of stars, intersecting solar level abundances at close to the Sun’s age of ~ 5 Gyrs, and descending at the oldest ages to $[\text{Fe}/\text{H}]$ of -1 dex. This result is fairly consistent, if not steeper in general, than that predicted for the solar vicinity by recent theoretical work (e.g. [Roškar et al. 2008a](#); [Minchev et al. 2013](#)). The scatter in metallicity vs. age is significant enough to make comparisons with the simulations difficult, especially since they typically show non-linearity in the relation toward older ages; however it is worth mentioning that [Roškar et al. \(2008a\)](#) show, in their simulated data, that an in-situ population in the solar vicinity, as opposed to one including radial migration, exhibits a steeper, and tighter, AMR. The bottom panel of Figure 9 is similar to the top, except showing the $[\text{Ti}/\text{Fe}]$ abundances. The slope is quite shallow, but positive, for young stars, and consistent with single star ages. We see a knee at around 9 Gyr, prior to which there is a rapid rise in α abundances with respect to $[\text{Fe}/\text{H}]$. The age at which this abundance knee is observed is the same age that appears to separate the abundance determined thin and thick disc stars seen in Figure 8.

One could argue about the presence of a knee in the $[\text{Fe}/\text{H}]$ distribution. If indeed present in these data, it is certainly a weak signature. The bi-modality of the alpha abundance relation with age, however, is unambiguous. Recently, [Bovy et al. \(2012\)](#) suggested that the Galaxy does not have a distinct two-component disc in terms of scale-height, but rather a smooth distribution, and that the $[\alpha/\text{Fe}]$ vs $[\text{Fe}/\text{H}]$ bimodality previously seen was merely a selection effect. The W-component AVR in the top right panel of Figure 7, seems to argue in favor of a smooth distribution, given the smooth monotonic heating signature seen, though we must note the kinematic selection of the data may preclude such analysis. The chemical evolution is clearly not smooth, however, and the disc appears to have two distinct components in the sense that something triggered a change in the mode of enrichment around 9 Gyrs ago. Given that stars of ages greater than 9 Gyrs are predominantly thick disc, this could be indicative of a separate star formation history for these two populations.

6 THE NATURE OF CHEMICALLY TAGGED GROUPS

The initial and operating assumption for much of this work has been that chemically tagged groups represent conatal groups of stars. In light of results from the previous sections, we revisit the interpretations introduced in Section 3.2 that aim to explain the seemingly large numbers of stars in this local sample that were tagged to groups. Four options were proposed which included unexpectedly high contamination levels in chemically tagged groups, open clusters as non-representative of typical Galactic star formation events, very poor mixing efficiencies within the disc, and finally homogeneity of chemical evolution on a Galactic scale as opposed to a local molecular cloud scale. We reiterate that the calibration used for determining the probability limits chemical tagging is based on open clusters, which have been shown to not exhibit an AMR (e.g. see [Pancino et al. 2010](#)), and are further at odds with our understanding of “typical” star formation due to the fact that we observe intermediate age and old open clusters, which presumably should have dispersed many millions or billions of years prior. Thus they may not be the best calibrator for field stars (unfortunately, there are no better calibrators at this point in time). Adding to that, the

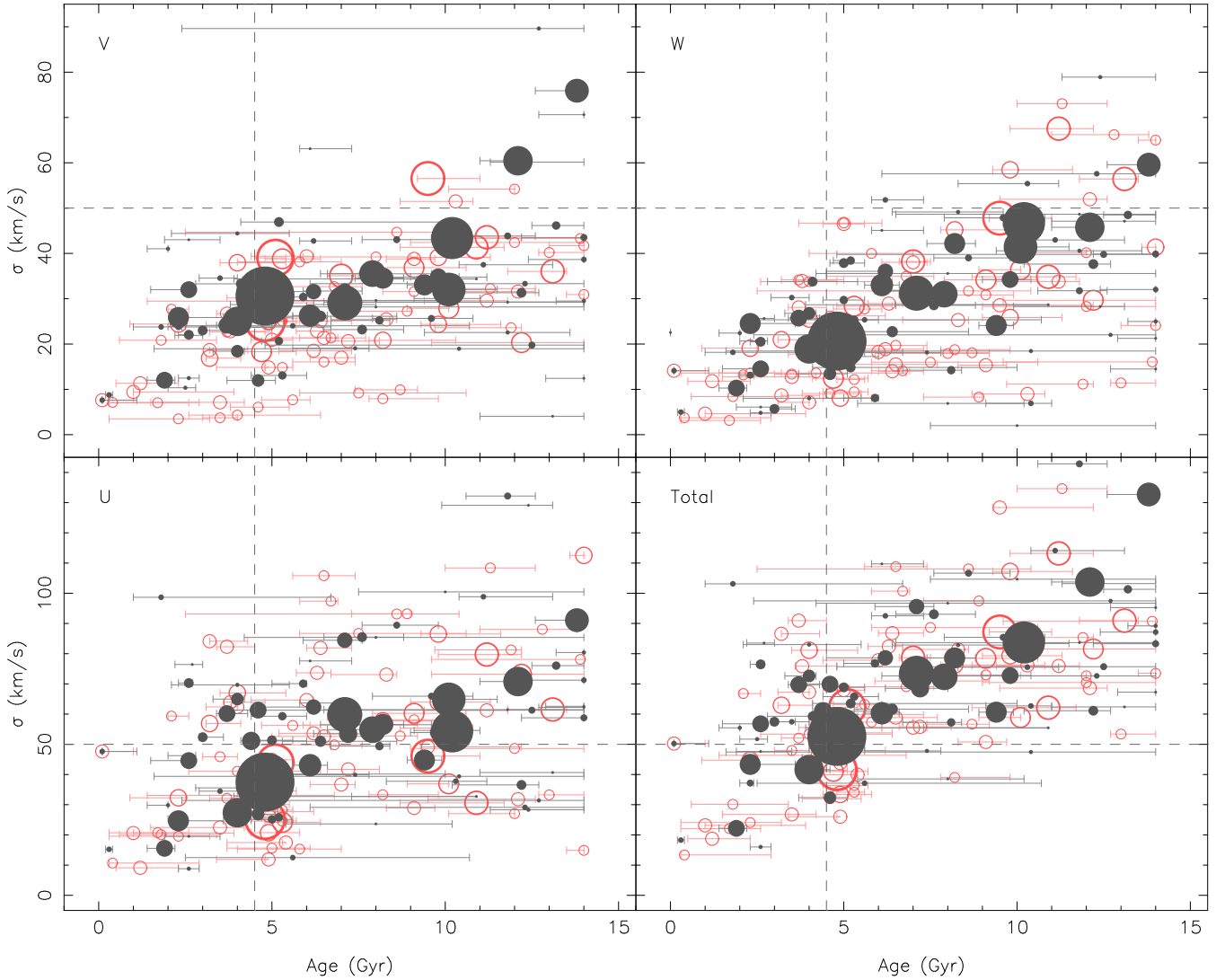


Figure 7. Age vs internal velocity dispersions of chemically tagged groups in the U, V, W components and the total dispersion, as indicated on the plots. Filled grey circles are groups tagged to $P_{lim} = 68\%$ threshold, open red circles are to the 90% threshold. The sizes of symbols represent relative sizes of groups. All groups plotted here have three or more members. The dashed axes at 4.5 Gyr and 50 km s^{-1} in each panel elucidate the difference in σ -scale of the top and bottom panels.

purely chemical approach to the empirical probability function ignores the *a-priori* probability of a pair of stars being born together in a given volume. In a Galaxy with few clusters that remained localized, the function would be weighted towards conatal groups, enhancing the ability to tag stars at a given chemical difference. In a galaxy with many clusters and efficient mixing, the function would be weighted towards distinct sites of formation, reducing or eliminating the ability to tag, in a given volume.

The consistency in our results with respect to the age-metallicity-velocity (AMVR) relations indicate that option number 1, noted in Section 3.2, cannot be wholly responsible. The fact that open clusters are seen to very old ages, and the lack of an age-metallicity relation amongst them, already indicates that they do not represent typical star formation events in the Galaxy. Therefore option number 2 is certainly possible, yet, again, the consistency in AMVR we find seems to indicate the group members have a relationship beyond their chemistry. Numerical Galaxy evolution simulations suggest that radial migration is widespread (Roškar et al.

2008b,a; Minchev et al. 2011), possibly even responsible for kinematically heating the thick disc (Loebman et al. 2011). Observational evidence of this process, however, is difficult to come by. Assuming this is the case would rule out option number 3, leaving 4 as the most likely candidate. This scenario could explain the AMVR, and would mean that a chemical signature, to the precision we are able to currently measure it, does not represent a single site of star formation, but rather the prevailing chemical abundance pattern during a Galactic epoch of star formation. Alternatively, making the assumption that chemically tagged groups represent conatal stars, we could make the conclusion that radial migration is not as strong a factor as simulations suggest.

In a blind chemical tagging experiment, with presently available data, there is no robust check one can do to ensure the correct assumptions went into linking groups. Qualifying the chemically tagged ages against established age relations in the literature is also problematic given the issues related to computing ages for individual stars. However, we find encouraging the consistency of these

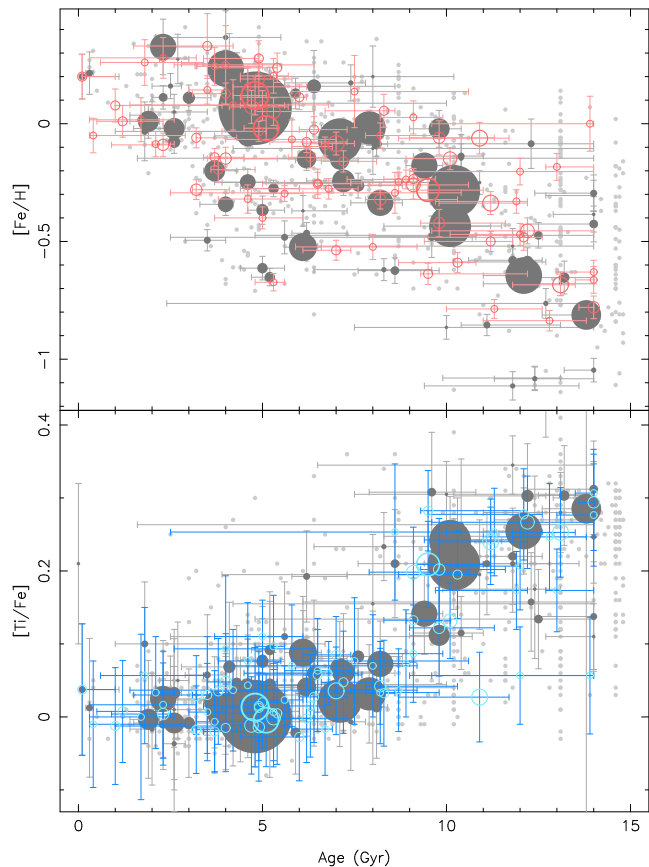


Figure 9. Age vs metallicity for coeval groups using chemically tagged ages and mean $[\text{Fe}/\text{H}]$ abundances. Filled grey circles are groups tagged to a $P_{lim} = 68\%$ threshold, red open circles are to the 90% threshold. The size of symbols represents the relative size of groups. All groups plotted here have three or more members. The light grey points show the individual stars which are members of a 68% tagged group with greater than three members, but with their single star age. The bottom panel is the same as the top but showing $[\text{Ti}/\text{Fe}]$ as a function of age (here the open symbols are blue). The trends are broadly consistent, except the coeval groups appear to exhibit a tighter trend and steeper drop off in $[\text{Fe}/\text{H}]$ beyond approximately 9 Gyrs, while the Ti abundances rapidly rise at the same cutoff.

results with the broad generalizations of how the Galaxy, and stars within it, evolved.

7 SUMMARY & CONCLUSIONS

We have performed the first ever blind chemical tagging experiment on a sample of 714 stars with high-resolution abundance measurements of 12 elements. Using the methodology in Mitschang et al. (2013) we linked chemically tagged groups in two probability regimes, $P_{lim} = 68$ and $P_{lim} = 90\%$, yielding 70 and 71 coeval group detections with an average of ~ 8 and ~ 4 stars each, amounting to 80 and 40% of stars in the entire sample tagged to associations with 3 or more members, respectively.

Several challenges present themselves. The seemingly large fraction of stars tagged would imply weak churning efficiencies if these groups represented discrete sites of star formation within a molecular clouds. Yet, evidence is mounting that these mixing processes are quite strong. Alternatively, the coeval groups may represent Galactic epochs of star formation, in which the nuclear

enrichment processes follow the same patterns regardless of position in the Galaxy, to within the tolerance of age measurements. The fact that open clusters are the only source of empirical calibration on the chemical tagging probability function is problematic, particularly for the latter interpretation. There is no doubt, however, that a calibration of the probability function using a large, homogeneously analyzed, open cluster sample, e.g., that from the Gaia-ESO Survey, will help to better understand the results of blind chemical tagging experiments.

Traditional stellar group membership criteria, i.e. those used to determine membership for globular and open clusters, do not apply to group finding via blind chemical tagging. Kinematic membership criteria for open clusters require very low internal velocity dispersions and common space motions, yet we have seen high dispersion amongst chemically tagged groups, and the patterns do not appear similar to Galactic moving groups. Kinematics may be loosely used as an additional parameter to group linking through the total internal velocity dispersion relation with age. It is unclear how useful this will be in practice. In most cases, the scatter in the isochrone of potential members is not enough to use those stellar parameters as a discriminator. In our sample, less than 10% of recovered groups exhibited obvious outliers in the CMD plane.

Additionally, our results indicate that stellar ages do not add another dimension to the chemical tagging group finding parameter space. This is especially true for the most common method of computed ages for single stars, isochrone fitting. Few of the detected coeval groups have pre-computed (single star) ages that are compatible with the age computed from the group. Although we cannot be definitive in the matching of stars to coeval groups, given the relations derived from chemically tagged ages, and the problems associated with isochrone fitting for single stars, chemical tagging may present a viable alternative to computing ages for stars in the samples of upcoming large scale surveys like GALAH and Gaia-ESO.

We have shown that the results of coeval group linking, in particular the abundance and kinematic relations with chemically tagged ages, are consistent with modern broad understanding of the nature of their evolution. The importance of accurate astrophysical ages cannot be overstated. Regardless of the interpretation of the groups, whether they represent discrete sites, or simply epochs of formation, these ages provide a powerful diagnostic, and the consistency observed here is encouraging looking forward to the upcoming large-scale chemical tagging experiments.

8 ACKNOWLEDGEMENTS

AWM gratefully acknowledges the Australian Astronomical Observatory for a PhD top-up scholarship grant which has, and will continue to support this work. The authors would like to thank members of the Macquarie University and Australian Astronomical Observatory joint Galactic archaeology group, Daniela Carollo, Valentina D’Orazi, and Sarah Martell for helpful discussions. AWM and DBZ thank Hans-Walter Rix at the Max-Planck Institute for Astronomy in Heidelberg, Germany for discussion and suggestions related to the interpretation of chemically tagged groups. DBZ acknowledges the support of Future Fellowship FT110100743 from the Australian Research Council. T.B. was funded by grant No. 621-2009-3911 from The Swedish Research Council. S.F. was partly funded by grants No. 621-2011-5042 from The Swedish Research Council.

References

- Abadi, M. G., Navarro, J. F., Steinmetz, M., & Eke, V. R. 2003, *ApJ*, 597, 21
- Anguiano, B., Freeman, K. C., Steinmetz, M., & Wylie de-Boer, E. 2013, in prep.
- Bensby, T., Feltzing, S., & Lundström, I. 2003, *A&A*, 410, 527
- Bensby, T., Feltzing, S., Lundström, I., & Ilyin, I. 2005, *A&A*, 433, 185
- Bensby, T., Feltzing, S., & Oey, M. S. 2013, arXiv:1309.2631
- Bensby, T., Adén, D., Meléndez, J., et al. 2011, *A&A*, 533, A134
- Bovy, J., Rix, H.-W., & Hogg, D. W. 2012, *ApJ*, 751, 131
- Bubar, E. J., & King, J. R. 2010, *AJ*, 140, 293
- Carretta, E., Bragaglia, A., Gratton, R. G., Lucatello, S., & D’Orazi, V. 2012, *ApJ*, 750, L14
- Casagrande, L., Schönrich, R., Asplund, M., et al. 2011, *A&A*, 530, A138
- De Silva, G. M., D’Orazi, V., Melo, C., et al. 2013, *MNRAS*, 431, 1005
- De Silva, G. M., Freeman, K. C., Asplund, M., et al. 2007a, *AJ*, 133, 1161
- De Silva, G. M., Freeman, K. C., Bland-Hawthorn, J., Asplund, M., & Bessell, M. S. 2007b, *AJ*, 133, 694
- De Silva, G. M., Freeman, K. C., Bland-Hawthorn, J., et al. 2011, *MNRAS*, 415, 563
- De Silva, G. M., Sneden, C., Paulson, D. B., et al. 2006, *AJ*, 131, 455
- Demarque, P., Woo, J.-H., Kim, Y.-C., & Yi, S. K. 2004, *ApJS*, 155, 667
- Feltzing, S., Bensby, T., & Lundström, I. 2003, *A&A*, 397, L1
- Feltzing, S., & Holmberg, J. 2000, *A&A*, 357, 153
- Feltzing, S., Holmberg, J., & Hurley, J. R. 2001, *A&A*, 377, 911
- Freeman, K., & Bland-Hawthorn, J. 2002, *ARA&A*, 40, 487
- Freeman, K. C., Bland-Hawthorn, J., SMG, & GALAH team. 2013, in prep.
- Fuhrmann, K. 1998, *A&A*, 338, 161
- Gilmore, G., & Reid, N. 1983, *MNRAS*, 202, 1025
- Gilmore, G., Randich, S., Asplund, M., et al. 2012, *The Messenger*, 147, 25
- Haywood, M. 2006, *MNRAS*, 371, 1760
- Høg, E., Fabricius, C., Makarov, V. V., et al. 2000, *A&A*, 355, L27
- Janes, K. A., Tilley, C., & Lynga, G. 1988, *AJ*, 95, 771
- Karlsson, T., Bland-Hawthorn, J., Freeman, K. C., & Silk, J. 2012, *ApJ*, 759, 111
- Lada, C. J., & Lada, E. A. 2003, *ARA&A*, 41, 57
- Loebman, S. R., Roškar, R., Debattista, V. P., et al. 2011, *ApJ*, 737, 8
- Minchev, I., Chiappini, C., & Martig, M. 2013, *A&A*, 558, A9
- Minchev, I., Famaey, B., Combes, F., et al. 2011, *A&A*, 527, A147
- Mitschang, A. W., De Silva, G., Sharma, S., & Zucker, D. B. 2013, *MNRAS*, 428, 2321
- Navarro, J. F., Abadi, M. G., Venn, K. A., Freeman, K. C., & Anguiano, B. 2011, *MNRAS*, 412, 1203
- Nordström, B., Andersen, J., Holmberg, J., et al. 2004, *PASA*, 21, 129
- Pancino, E., Carrera, R., Rossetti, E., & Gallart, C. 2010, *A&A*, 511, A56+
- Pompéia, L., Masseron, T., Famaey, B., et al. 2011, *MNRAS*, 415, 1138
- Quinn, P. J., Hernquist, L., & Fullagar, D. P. 1993, *ApJ*, 403, 74
- Reddy, B. E., Lambert, D. L., & Allende Prieto, C. 2006, *MNRAS*, 367, 1329
- Reddy, B. E., Tomkin, J., Lambert, D. L., & Allende Prieto, C. 2003, *MNRAS*, 340, 304
- Rix, H.-W., & Bovy, J. 2013, ArXiv e-prints
- Rocha-Pinto, H. J., Maciel, W. J., Scalo, J., & Flynn, C. 2000, *A&A*, 358, 850
- Roškar, R., Debattista, V. P., & Loebman, S. R. 2013, *MNRAS*, 433, 976
- Roškar, R., Debattista, V. P., Quinn, T. R., Stinson, G. S., & Wadsley, J. 2008a, *ApJ*, 684, L79
- Roškar, R., Debattista, V. P., Stinson, G. S., et al. 2008b, *ApJ*, 675, L65
- Sellwood, J. A., & Binney, J. J. 2002, *MNRAS*, 336, 785
- Soderblom, D. R. 2010, *ARA&A*, 48, 581
- Soubiran, C., Bienaymé, O., Mishenina, T. V., & Kovtyukh, V. V. 2008, *A&A*, 480, 91
- Steinmetz, M., Zwitter, T., Siebert, A., et al. 2006, *AJ*, 132, 1645
- Tabernero, H. M., Montes, D., & Gonzalez Hernandez, J. I. 2012, *A&A*, in press, ArXiv:1205.4879
- Ting, Y. S., Freeman, K. C., Kobayashi, C., de Silva, G. M., & Bland-Hawthorn, J. 2012, *MNRAS*, 421, 1231
- Yanny, B., Rockosi, C., Newberg, H. J., et al. 2009, *AJ*, 137, 4377